

Available online at www.sciencedirect.com**ScienceDirect**

Procedia Technology 25 (2016) 1038 – 1048

Procedia
Technology

Global Colloquium in Recent Advancement and Effectual Researches in Engineering, Science and Technology (RAEREST 2016)

Parametric Optimization of MIG Welding on 316L Austenitic Stainless Steel by Grey-Based Taguchi Method

Nabendu Ghosh^{*a}, Pradip Kumar Pal^b, Goutam Nandi^c

^{*a}Ph.D student, Mechanical Engineering Department, Jadavpur University, Kolkata 700032, WB, INDIA

^{b,c}Professor, Mechanical Engineering Department, Jadavpur University, Kolkata 700032, WB, INDIA

Abstract

In the present work, visual inspection and X-ray radiographic test has been conducted in order to detect surface and sub-surface defects of weld specimens made of AISI 316L austenitic stainless steels. Effect of current, gas flow rate and nozzle to plate distance on quality of weld in metal inter gas arc welding of AISI 316L austenitic stainless steel has been studied in the present work through experiments and analyses. Butt welded joints have been made by using several levels of current, gas flow rate and nozzle to plate distance. The quality of the weld has been evaluated in terms of yield strength, ultimate tensile strength and percentage of elongation of the welded specimens. The observed data have been interpreted, discussed and analyzed by using Grey - Taguchi methodology

© 2016 The Authors. Published by Elsevier Ltd. This is an open access article under the CC BY-NC-ND license (<http://creativecommons.org/licenses/by-nc-nd/4.0/>).

Peer-review under responsibility of the organizing committee of RAEREST 2016

Keywords: MIG welding, AISI 316L Austenitic stainless steel, Visual Inspection, X-ray Radiographic Inspection, Tensile Test, Taguchi-Grey Relational Technique

^{*a} Corresponding author. Tel: 9433449315.

^{*a} E-mail address: nabendu2003_ghosh@yahoo.co.in

1. INTRODUCTION

The S.S 316L is a chromium-nickel-molybdenum austenitic stainless steel developed to provide improved corrosion resistance to S.S 304/304L in moderately corrosive environments. The addition of molybdenum improves general corrosion and chloride pitting resistance [1-3]. 316 stainless steel is selected over other materials because of its distinct properties, cheaper cost and its availability in the market. 316 stainless steel used is a boiler grade steel used in pressure vessels. This grade has high corrosion resistance and can be operated at elevated temperature.[9] Type 316 stainless steel is widely used in application requiring corrosion resistance superior to Type 304, or good elevated temperature strength. Typical uses include exhaust manifolds, furnace parts, heat exchangers, jet engine parts, pharmaceutical and photographic equipment, valve and pump trim, chemical equipment, digesters, tanks, evaporators, pulp, paper and textile processing equipment Weld quality mainly depends on features of bead geometry, mechanical-metallurgical characteristics of the weld as well as on various aspects of weld chemistry and these features are expected to be greatly influenced by various input parameters like current, voltage, electrode stick-out, gas flow rate, edge preparation, position of welding, welding speed and many more in metal inert gas (MIG) welding. Moreover, the cumulative effect of the mentioned quality indices determines the extent of joint strength that should meet the functional aspects of the weld in practical field of application. Therefore, preparation of a satisfactory good quality weld seems to be a challenging job. The welding investigators have always been in search for better quality of weldment. Welding of austenitic stainless steel in general, and MIG welding of such steel in particular, can well be considered as one of the areas where more extensive research may contribute, in a significant way, to the precise control of welding procedure for better and acceptable quality of weldment. Researchers had done investigations on joining the 316L austenitic stainless steel materials with use of MIG welding technique, those are discussed below: Hu et al [1] employed a high-precision magnetic sensor to detect the weld defects in aluminium friction stir welds. Lee et al. [2] have used the Taguchi method and regression analysis in order to optimize Nd-YAG laser welding parameters. Laser butt-welding of a thin plate of magnesium alloy using the Taguchi method has been optimized by Pan et al. [3] Ibrahim et al. [4] investigated the effects of robotic GMAW process parameters on welding penetration, hardness and microstructural properties of mild steel weldments of 6mm plate thickness. Murugan and Parmar [5] used a four-factors 5-levels factorial technique to predict the weld bead geometry (penetration, reinforcement, width and dilution %) in the deposition of 316L stainless steel onto structural steel IS2062 using the MIG welding process. Rosado et al [6] utilized the eddy currents probe to detect the imperfections in friction stir welds of aluminum. Senthil Kumar et al. [7] developed mathematical models by regression analysis to predict the effects of pulsed current tungsten inert gas welding parameters on tensile properties of medium strength AA 6061 aluminium alloy. Seshank et al. [8] used ANN and Taguchi method to analyze the effect of pulsed current GTAW process parameters on bead geometry of aluminium bead-on-plate weldment. Sittichai et al. [9] investigated the effects of shielding gas mixture, welding current and welding speed on the ultimate tensile strength and percentage elongation of GMA Welded. Sourav Datta et al. [10] used Taguchi approach followed by grey relational analysis to solve multi –response optimization problem in submerged arc welding. Juang and Tarng [11] have adopted a modified Taguchi method to analyze the effect of each welding process parameter (arc gap, flow rate, welding current and speed) on the weld pool geometry (front and back height, front and back width) and then to determine the TIG welding process parameters combination associated with the optimal weld pool geometry. Tarng and Yang [12] reported on the optimization of weld bead geometry in GTAW by using the Taguchi method. Tarng et al. [13] applied the modified Taguchi method to determine the process parameters for optimum weld pool geometry in TIG welding of stainless steel. Tarng et al. [14] also worked on the use of grey-based Taguchi method to determine optimum process parameters for submerged arc welding (SAW) in hard facing with consideration of multiple weld qualities. Yilmaz and Uzun [15] compared the results obtained from destructive tests for mechanical properties of austenitic stainless steel. (AISI 304L and AISI 316L plates of 5 mm thickness) joints welded by GMAW and GTAW process. The joints were made by GMAW process using ER 316 L Si filler metal and by GTAW process using ER 308L and ER 316L filler metals. In the present work the effects of current, gas flow rate and nozzle to plate distance on ultimate tensile strengths, yield strength and percentage of elongation of butt welded joints of austenitic stainless steel have been experimented and analyzed through Taguchi-based grey relational methodology.

2. EXPERIMENTAL PLAN, SET UP AND PROCEDURE

Butt welding of AISI 316L austenitic stainless steel: 60mm x 100mm x 3mm thick, have been done using the MIG welding machine make: ESAB AUTO K400. Taguchi design has been adopted in order to identify optimal parametric combination for desired quality of weld. Total of 9 butt welded specimens have been obtained using 3 levels of current , 3 levels of gas flow rate and 3 level of nozzle to plate distance based on L9 Taguchi’s Orthogonal Array Design of experiment. The interaction effects have not been considered in the present work. The filler rod used has been ER 316L. Welding process parameters and their levels, and design matrix are shown in **Table 1** and **Table 2** respectively. Chemical Composition of Base Plate and Filler metal is shown in **Table3**.

Table 1. Welding process parameters and their levels (Domain of experimentation) for L9 Taguchi’s Orthogonal Array Design of experiment

FACTORS	SYMBOL	UNIT	LEVELS		
			1	2	3
Welding Current	C	A	100	112	124
Gas Flow rate	F	l/min	10	15	20
Nozzle to plate Distance	S	mm	9	12	15

Table 2. Design matrix based on L9 Taguchi Orthogonal Array design of experiment

Sample. No	Welding parameters		
	Welding Current (A)	Gas flow rate (l/min)	Nozzle to plate Distance (mm)
1	1	1	1
2	1	2	2
3	1	3	3
4	2	1	2
5	2	2	3
6	2	3	1
7	3	1	3
8	3	2	1
9	3	3	2

Table3. The chemical composition of stainless steel grade

Base Plate	Composition wt%										
	C	Mn	Si	P	Cr	Ni	Mo	Cu	Al	S	T
316L	0.03	1.47	0.58	0.025	18.33	8.33	0.2	0.19	0.01	0.01	----
Filler Metal											
316L	0.02	1.68	0.53	0.012	19.45	9.22	0.116	0.082	0.01	0.03	----

Butt welded joints being done under varied input parameters, visual inspection and X-ray radiographic test of all welded specimens has been made. After visual inspections and X-ray radiographic test, tensile test specimens have been prepared from the welded joints, by cutting/machining. During cutting/machining of the tensile test specimens, small cut- outs have been taken. These cut pieces have then been ground, polished and etched for studying microstructures. Results of Visual inspection and X-ray radiographic tests are reported in section3 and 4 respectively. The Photographic view of welded sample is shown in **Figure1**.

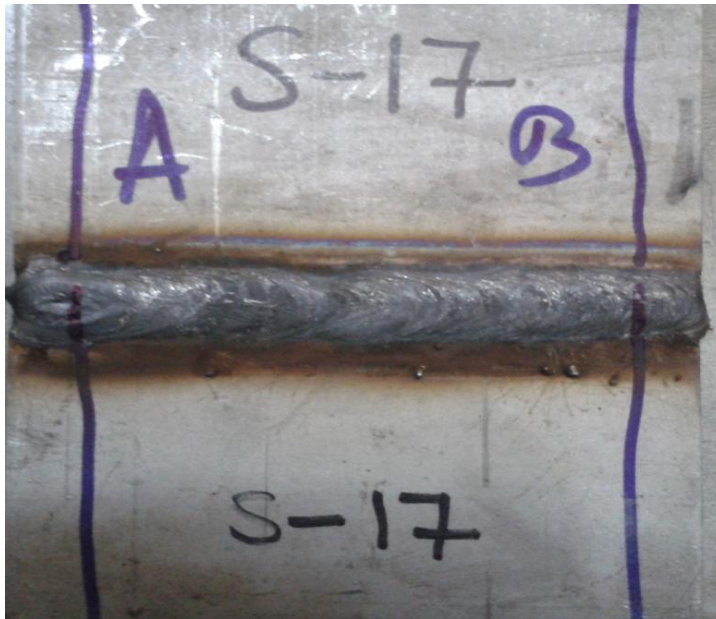


Figure1. The Photographic view of welded sample

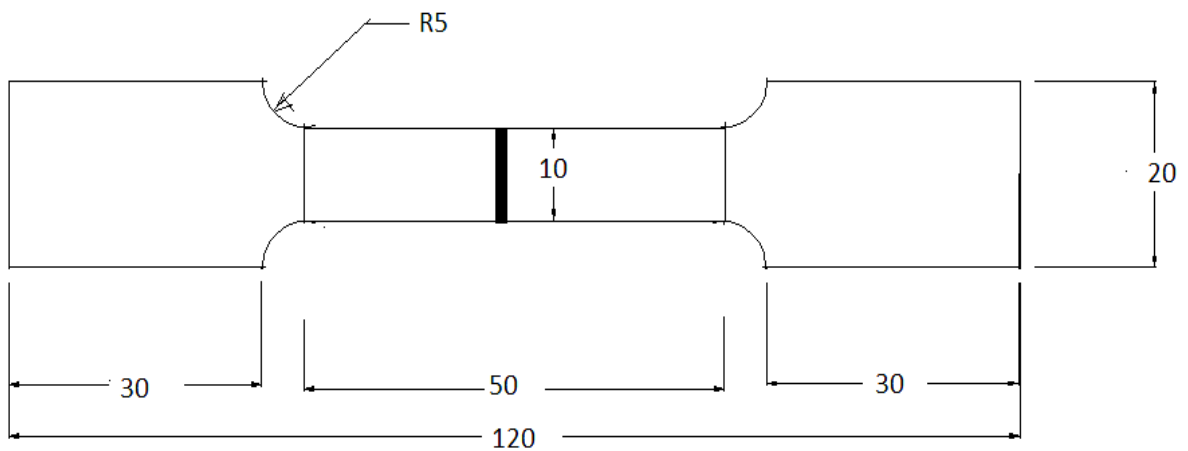


Figure2. Tensile test diagram for gas metal arc welding

Butt welded joints being done under varied input parameters, tensile test specimens have been prepared from the welded joints, by cutting/machining. The tensile test specimens have been tested on tensile testing machine INSTRON as per ASTM standard. Tensile Test diagram is shown in **Figure2**

3. RESULTS OF VISUAL INSPECTION OF WELDMENT AND DISCUSSION

For visual inspection, the weld surface is observed with the naked eye, in order to detect the surface defects of the weldment. The observed result of visual inspection is shown in Table 4

Table 4 Observed result of visual inspection of weld specimen

sample no.	Welding Current (A)	Gas Flow Rate (l/min)	Nozzle to plate distance (mm)	Result of visual inspection
1	100	10	9	NO DEFECTS
2	100	15	12	EXCESSIVE DEPOSITION, SPATTER
3	100	20	15	NO DEFECTS
4	112	10	12	NO DEFECTS
5	112	15	15	SPATTER
6	112	20	9	NO DEFECTS
7	124	10	15	UNEVEN PENETRATION
8	124	15	9	NO DEFECTS
9	124	20	12	SPATTER ,EXCESSIVE DEPOSITION

it is found from this table that for certain welding conditions; no defect has been observed. These are for the sample no.1, 3, 4, 6 & 8. Blow holes and undercut, spatter, uneven penetrations are the types of defects which are found in other samples.

Spatter found only for sample nos 2, 5 and 9, is caused possibly due to damp filler rod or arc blow or bubble of gas being entrapped in the molten globule of metal expanding with great violence and projecting small drops of metal outside the arc seam. High current might be the reason, but no high current is used for samples 2. Too low or too high current and/or faster travel speed might have caused blow holes. Incorrect welding technique attempting stringer or weaved beads, unclean job surface, damp filler rod are also considered as some reasons for which blow holes or porosity may form. Again, blow holes and porosity might have resulted from gas getting entrapped in solidifying metal, larger arc etc. In some samples undercuts have been found, which might have been caused by improper joint geometry or because of incorrect combination of current, gas flow rate and nozzle to plate distance. Other possible reasons behind undercut are: faster arc travel speed during welding or larger arcs, wrong filler rod

4. RESULTS OF X-RAY RADIOGRAPHIC TESTS OF WELDMENT AND DISCUSSION

X- Ray radiographic tests have been conducted for all the 9 samples by XXQ-2005 X-Ray flaw detector. The copies of radiography films of few samples are included in Figures.3-4

Table 5 Result of X-ray radiographic test

sample no.	Welding Current (A)	gas flow rate (l/min)	Nozzle to plate distance (mm)	Result of X-ray radiographic tests
1	100	10	9	NO DEFECTS
2	100	15	12	LACK OF FUSION, POROSITY
3	100	20	15	NO DEFECTS
4	112	10	12	NO DEFECTS
5	112	15	15	POROSITY
6	112	20	9	NO DEFECTS
7	124	10	15	POROSITIES
8	124	15	9	NO DEFECTS
9	124	20	12	POROSITIES

Lack of fusion at root or wall has occurred possibly due to improper setting of the current, improper cleaning, faster arc travel speed, presence of oxides, scale and other impurities which do not permit the deposited metal to fuse

properly with the base metal. Too low heat input does not ensure proper melting of the weld deposit. With too high heat input, the weld pool becomes too large and starts to flow away in the area in front of the arc which prevents melting of the base metal .lack of fusion found in sample no.2.



Figure3: X-ray radiographic film for Sample no. 06



Figure4: X-ray radiographic film for Sample no. 03

Porosity has been found in sample nos. 5, 7 & 9 which may have resulted from gas being entrapped in the solidifying metal. Porosity can be a significant problem which is very tough to solve. The biggest causes are probably contamination of the shielding gas, followed by filler metal and base metal contamination. If the results of visual inspection and X-ray radiographic tests are compared, some consistency in the findings can be noticed.

Visual and X-ray radiographic tests also indicate that sample nos. 1, 3, 4, 6 and 8 has got no significant defect – thus causing reasons for good performance of the sample under tensile testing. It has been found from the table5 that no defects has been found under low current, medium gas flow rate and low nozzle to plate distance,

5. RESULTS OF TENSILE TEST AND DISCUSSION

The tensile test specimens, prepared corresponding to L9 Taguchi Orthogonal Array experiments, have been tested for tensile strengths and the results obtained are given in **Table 6**.

Table 6. Tensile tests result as per L9 Taguchi Orthogonal Array Design of experiment

SAMPLE NO.	YIELD STRENGTH (MPa)	ULTIMATE TENSILE STRENGTH(MPa)	PERCENTAGE OF ELONGATION (%)
------------	----------------------	--------------------------------	------------------------------

BASE PLATE	301.6119	573.7524	65.048
1	321.1262	550.0938	31.212
2	317.9749	552.0211	34.643
3	322.7427	591.1774	54.539
4	288.8381	518.2146	33.023
5	250.227	432.3345	18.53
6	264.2308	481.4142	33.072
7	242.4277	426.2334	19.524
8	246.7417	484.9734	42.774
9	233.0469	450.9941	28.403

The **Table 6** indicates that for many of the welded samples test results are satisfactory. The best result is obtained for the sample no.3 (Corresponding to current 100 A, flow rate 20 l/min and nozzle to plate distance 15 mm). For this sample yield strength=322.7427MPa ultimate tensile strength =591.1774MPa percentage of elongation =54.539. The worst result in tensile testing has been obtained for the sample no. 7 (corresponding to current 124 A, gas flow rate 10 l/min and nozzle to plate distance 15mm). For this sample yield strength=242.4277and ultimate tensile strength = 426.23343MPa and percentage of elongation =19.524

6. ANALYSES AND OPTIMIZATION OF ULTIMATE TENSILE STRENGTH, YIELD STRENGTH AND PERCENTAGE OF ELONGATION BY GREY TAGUCHI METHOD

6.1 TAGUCHI METHOD

Taguchi's method is developed by Dr. Genichi Taguchi, a Japanese quality management consultant. Taguchi method uses a statistical measure of performance called signal-to-noise ratio that takes both the mean and the variability into account. The method explores the concept of quadratic quality loss function. The S/N ratio is the ratio of the mean (signal) to the standard deviation (noise). The ratio depends on the quality characteristics of the product/process to be optimized. The standard S/N ratios generally used are Nominal-is-Best (NB), lower-the-better (LB) and Higher-the-Better (HB). The optimal setting is the parametric combination, which has the highest S/N ratio. However, traditional Taguchi method cannot solve multi-objective optimization problem. This can be achieved by grey based Taguchi method. The grey system theory proposed by Deng in 1982 has been proven to be useful for dealing with poor, incomplete, and uncertain information. The grey relational analysis based on grey system theory can be used to solve complicated inter-relationships among multiple performance characteristics effectively.

Taguchi's S/N Ratio for (NB) Nominal-the-best

$$\eta = 10 \ln_{10} \frac{1}{n} \sum_{i=1}^n \frac{\mu^2}{\sigma^2} \quad (1)$$

Taguchi's S/N Ratio for (LB) Lower-the-better

$$\eta = -10 \ln_{10} \frac{1}{n} \sum_{i=1}^n y_i^2 \quad (2)$$

Taguchi's S/N Ratio for (HB) Higher-the-better

$$\eta = -10 \ln_{10} \frac{1}{n} \sum_{i=1}^n \frac{1}{y_i^2} \quad (3)$$

6.2 GREY RELATIONAL ANALYSIS

In grey relational analysis, experimental data i.e. measured features of quality characteristics of the product are first normalized ranging from zero to one. This process is known as grey relational generation. Next, based on normalized experimental data, grey relational coefficient is calculated to represent the correlation between the desired and actual experimental data. Then overall grey relational grade is determined by averaging the grey relational coefficient corresponding to selected responses. The overall performance characteristic of the multiple response process depends on the calculated grey relational grade. This approach converts a multiple- response- process optimization problem into a single response optimization situation, with the objective function in overall grey relational grade. The optimal parametric combination is then evaluated by maximizing the overall grey relational grade.

A linear normalization of the experimental data is performed in the range between zero and unity, which is also called the grey relational generating.

For Higher-the-Better (HB) criterion, the normalized data can be expressed as;

$$x_i(k) = \frac{y_i(k) - \min y_i(k)}{\max y_i(k) - \min y_i(k)} \tag{4}$$

where $x_i(k)$ is the value after the grey relational generation, $\min y_i(k)$ is the smallest value of $y_i(k)$ for the k th response, and $\max y_i(k)$ is the largest value of $y_i(k)$ for the k th response. An ideal sequence $x_0(k)$ is for the responses. The purpose of grey relational grade is to reveal the degrees of relation between the sequences says, $[x_0(k)$ and $x_i(k), i=1,2,3,\dots,16]$.

Normalization of experimental data is shown in **Table 7**. (Based on equation (1) – larger the better criterion).

Table 7. Normalization of experimental data based on L9 Taguchi Orthogonal Array design of experiment

SAMPLE NO.	YIELD STRENGTH (MPa)	ULTIMATE TENSILE STRENGTH (MPa)	PERCENTAGE OF ELONGATION (%)
1	0.98197	0.75093	0.35219
2	0.94684	0.76261	0.44747
3	1.00000	1.00000	1.00000
4	0.62200	0.55765	0.40248
5	0.19154	0.03699	0.00000
6	0.34766	0.33455	0.40384
7	0.10458	0.00000	0.02760
8	0.15268	0.35612	0.67328
9	0.00000	0.15012	0.27418

The grey relation coefficient $\xi_i(k)$ can be calculated as

$$\xi_i(k) = \frac{\Delta_{\min} + \theta \Delta_{\max}}{\Delta_{0i}(k) + \theta \Delta_{\max}} \tag{5}$$

Where $\Delta_{0i} = \| x_0 - x_i(k) \|$ difference of the absolute value $x_0(k)$ and $x_i(k)$; θ is the distinguishing coefficient $0 \leq \theta \leq 1$; Grey relation Coefficient and Grey relational grade are shown in **Table 8**.

After averaging the grey relation coefficients, the grey relational grade γ_i can be computed as:

$$\gamma_i = \frac{1}{n} \sum_{k=1}^n \xi_i(k) \tag{6}$$

where n = number of process responses. The higher value of grey relational grade corresponds to intense relational

degree between the reference sequence $x_0(k)$ and the given sequence $x_i(k)$. The reference sequence $x_0(k)$ represents the best process sequence. Therefore, higher grey relational grade means that the corresponding parameter combination is closer to the optimal.

Table 8. Grey relation coefficient and Grey relational grade

SAMPLE NO.	Grey relation coefficient			Grey relational grade
	YIELD STRENGTH (MPa)	ULTIMATE TENSILE STRENGTH (MPa)	PERCENTAGE OF ELONGATION(%)	
1	0.96520	0.66749	0.43561	0.68944
2	0.90390	0.67807	0.47505	0.68567
3	1.00000	1.00000	1.00000	1.00000
4	0.56948	0.53059	0.45557	0.51855
5	0.38213	0.34176	0.33333	0.35241
6	0.43390	0.42902	0.45614	0.43969
7	0.35832	0.33333	0.33958	0.34374
8	0.37111	0.43711	0.60480	0.47100
9	0.33333	0.37040	0.40789	0.37054

With the help of Response graph for mean grey relational grade (**Figures 5**) optimum parametric combination has been determined. The optimal factor setting becomes **C1F3S3** (i.e. welding current = 100 A, Gas flow rate = 20l/min and Nozzle to plate distance = 15mm)

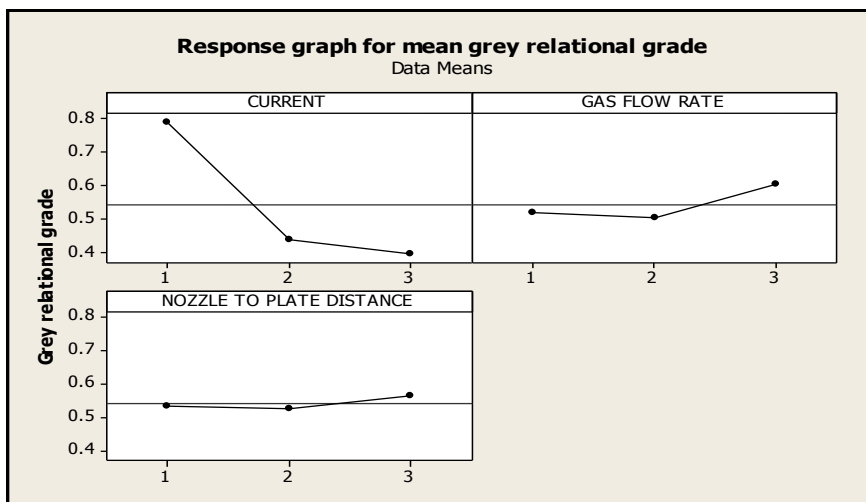


Figure5: Response graph for mean grey relational grade

Table 9: Response table for Grey relational grade value

Level	Current (A)	Gas flow rate (l/min)	Nozzle to plate distance (mm)
1	0.7917	0.5172	0.5334
2	0.4369	0.503	0.5249
3	0.3951	0.6034	0.5654
Delta	0.3966	0.1004	0.0405
Rank	1	2	3

Analysis of Variance for overall grey relation grade is shown in **Table 10**.

Table 10. Analysis of Variance for overall grey relation grade

	DF	Seq SS	Adj SS	Adj MS	F	P	Percentage of contribution
WELDING CURRENT	2	0.21923	0.21923	0.10962	2.42	0.292	59.58
GAS FLOW RATE	2	0.00595	0.00595	0.00298	0.07	0.938	1.617
NOZZLE TO PLATE DISTANCE	2	0.05228	0.05228	0.02614	0.58	0.634	14.2
Error	2	0.09049	0.09049	0.04525			
Total	8	0.36795					

The current appears to be more significant. Current is always an important parameter in any arc welding process. Both high and low currents give rise to several advantages and disadvantages. Proper current setting provides desired fusion, penetration and energy input. Energy input, energy input rate and the related heating and cooling cycles associated in any arc-welding process finally decides the metallurgical quality of weld and heat affected zone.

7. RESULTS OF CONFIRMATORY TEST

The results of confirmatory test are shown in **Table 11**. It is found that prediction of optimal parameter setting is valid.

Table 11. Results of Confirmatory Test

Level	Optimal Factors		
	Initial Condition	Prediction	Experiment
Level	C1F2S2	C1F3S3	C1F3S3
Yield Strength	317.9749		323
Ultimate Tensile strength	552		594
% of elongation	34.53		55
Grey Relational Grade	0.68567	0.878043	0.88042

Improvement of Grey relational grade:0.19475

8. CONCLUSIONS

Following conclusions are drawn in respect of MIG welding of AISI 316L austenitic stainless steel.

- Results of visual inspection indicate that undercut, blow holes and spatter have been found in few samples, uneven deposition, and excessive penetration have also been found in some samples.
- Results of X-ray radiography test indicate: lack of penetration, low – level porosity and lack of fusion in some of the samples.
- Results of visual inspection and X-ray radiographic tests are compared, some consistency are founds
- The best result is obtained for the sample no.3 (Corresponding to current 100 A, flow rate 20 l/min and nozzle to plate distance 15mm). The worst result in tensile testing has been obtained for the sample no. 7 (corresponding to current 124 A, gas flow rate 10 l/min and nozzle to plate distance 15).
- Current is found to be more significant than gas flow rate and nozzle to plate distance in influencing the strength of the joint.
- Optimization of the process parameters has been done by using Grey – Taguchi methodology; optimum parametric combination has been determined. The optimal factor setting becomes **C1F3S3** (i.e. welding current = 100A, Gas flow rate = 20l/min and Nozzle to plate distance =15mm).

9. REFERENCES

- [1] B, Hu., R, Yu., and H, Zou., Magnetic non-destructive testing methods for thin – plates aluminium alloys. *NDT&E International* 47: 66-69 (2012)
- [2] H. K., Lee, H. S., Han, K. J., Son, and S. B. Hong., Optimization of Nd-YAG laser welding parameters for sealing small titanium tube ends. *J. of Materials Science and Engineering*, Vol. A415, pp. 149-155 (2006).
- [3] L. K., Pan, C. C., Wang, Y. C., Hsiao and K. C., Ho, Optimization of Nd-YAG laser welding onto magnesium alloy via Taguchi analysis. *J. of Optics & Laser Technology*, Vol. 37, pp. 33-42 (2004)
- [4] Ibrahim, I. Z., et al., The effect of Gas Metal Arc Welding (GMAW) processes on different welding parameters. *Procedia Engineering* 41:1502-1506 (2012)
- [5] N. Murugan and R. S. Parmar., effects of MIG process parameters on the geometry of the bead in the automatic surfacing of stainless steel. *J. of Materials Processing Technology*, Vol. 41, pp. 381-398 (1994)
- [6] Rosado et al., Advanced technique for non-destructive testing of friction stir welding of metals. *Journal of Measurement* 43: 1021-1030 (2010)
- [7] Senthil Kumar, T., et al., Influences of pulsed current tungsten inert gas welding on the tensile properties of AA 6061 aluminium alloy. *Materials and Design* 28: 2080-2092 (2007)
- [8] Seshank, K., et al., Prediction of bead geometry in pulsed current gas tungsten arc welding of aluminium using artificial neural networks. *Proceedings of international conference on information and knowledge engineering, IKE*; June 23–26, Las Vegas [NV], USA: 149–53 (2003)
- [9] Sittichai, K., Santirat, N., and Sompong, P., A study of gas metal arc welding affecting mechanical properties of austenitic stainless steel AISI 304. *World Academy of Science, Engineering and Technology*: 61:402–405 (2012)
- [10] Datta S, Bandyopadhyay A, Pal P K, Grey-based taguchi method for optimization of bead geometry in submerged arc bead –on-plate welding. *Int J Adv Manuf Technol* 39:1136–1143 (2008)
- [11] S. C. Juang and Y. S. Tarng. , Process parameters selection for optimizing the weld pool geometry in the tungsten inert gas welding of stainless steel. *J. of Materials Processing Technology*, Vol. 122, 2002, 33-37 (2002)
- [12] Tarng YS, Yang WH., Optimization of the weld bead geometry in gas tungsten arc welding by the Taguchi method. *Int J Adv Manuf Technol* 14: 549–554 (1998)
- [13] Tarng YS, Yang WH, Juang SC, The use of fuzzy logic in the Taguchi method for the optimisation of the submerged arc welding process. *Inter J Adv Manuf Technol* 16: 688–694 (2000)
- [14] Tarng YS, Juang SC, Chang CH, The use of grey-based Taguchi methods to determine submerged arc welding process parameters in hard facing. *J Mater Process Technol* 128 (1–3):1–6 (2002)
- [15] Yilmaz, R., and Uzun, H., Mechanical properties of austenitic stainless steels welded by GMAW and GTAW. *Journal of Marmara for Pure and Applied Sciences* 18: pp. 97-113 (2002)
- [16] R.S. Parmar, *Welding Processes and Technology*, 2nd edition, Khanna Publications, New Delhi (1997)
- [17] O.P. Khanna, *Welding Technology*, Dhanpat Rai & Sons, (1986)
- [18] A. Ghosh, & A.K. Mallik, *Manufacturing Science*, East-West Press Private Limited, New Delhi (2008)